Chemical Physics Impact 8 (2024) 100521

Contents lists available at ScienceDirect

Chemical Physics Impact

journal homepage: www.sciencedirect.com/journal/chemical-physics-impact

Full Length Article

# Investigation on the corrosion inhibition efficiency of 2, 4-diphenyl-3-aza bicyclo[3.3.1] nonan-9-one in carbon steel immersed in acidic media

H. Mohamed Kasim Sheit [a,*], K.S. Mohan [b,*], K.V. Gunavathy [c], S.S. Syed abuthahir [a], M. Varusai Mohamed [a], P. Subhapriya [d], A. Samsathbegum [a], G . Hema Sindhuja [a]

[a] PG and Research, Department of Chemistry, Jamal Mohamed College (Autonomous), Affiliated to Bharathidasan University, Tiruchirappalli, Tamil Nadu 620 020, India

[b] Department of Physics, Nandha Engineering College (Autonomous), Erode, Tamil Nadu 638 052, India

[c] Thin Film Research Centre, Kongu Engineering College (Autonomous), Erode, Tamil Nadu 638 060, India

[d] Department of Chemistry, Bannari Amman Institute of Technology (Autonomous), Erode, Tamil Nadu 638 401, India

ARTICLE INFO

*Keywords:*
Corrosion inhibition
Acidic medium
Carbon steel
Anti corrosion efficiency
2, 4-diphenyl-3-azabicyclo[3.3.1] nonan-9-one
DFT

ABSTRACT

The current research investigates the corrosion resistant efficiency of 2,4-diphenyl-3-azabicyclo[3.3.1] nonan – 9–one (PABN) as inhibitor in carbon steel in 0.5 M $H_2SO_4$ environment through experimental and theoretical approaches. The weight loss methodology demonstrates that 0.10 ppm of nonan-9-one compound effectively inhibits corrosion in carbon steel submerged in an acidic environment with an efficiency of inhibition as high as 97.2 %. The polarization studies reveals the function of the compound as an inhibitor at the anodic site, influencing the kinetics of carbon steel corrosion effectively. Impedance spectra under alternating current conditions elucidate the influence of the protective film formed by the action of PABN compound on the electrical behavior and corrosion resistance in carbon steel material. This existence of the protective film composed of carbon steel and PABN compound is affirmed through different techniques such as SEM, EDX and AFM. The DFT analysis anticipates the interaction patterns of the inhibitor with the surface of carbon steel using quantum chemical calculations, analyzing the molecular interactions between the molecules of the inhibitor and the surface of carbon steel, providing insights into PABN's corrosion inhibitory properties.

## 1. Introduction

Carbon steel is a predominant alloy of iron and carbon with trace elements holding a crucial position in engineering and manufacturing with exemplifying versatility and indispensability. Renowned for its adaptability, carbon steel can be easily shaped rendering it as a preferred material for constructing a myriad of structures and components. Its exceptional strength and durability make it suitable for demanding applications in construction, automotive manufacturing, and infrastructure projects contributing to the creation of robust and enduring structures. Additionally, carbon steel's cost-effectiveness positions it favourably in large-scale projects, while its machinability and weldability facilitate efficient manufacturing processes [1–3]. Embodying eco-friendly practices, carbon steel is highly recyclable, aligning with global sustainability efforts. With a wide array of uses spanning from construction beams and automotive components to pipelines and industrial machinery, carbon steel stands as an essential material. The implementation of anti-corrosion measures in carbon steel is imperative to counteract the inherent vulnerability of the material to corrosion [4,5]. By preserving structural integrity, extending service life, and mitigating economic costs associated with premature failures, anti-corrosion strategies contribute significantly to the reliability and efficiency of carbon steel structures and components [6,7].

Several compounds were synthesised and explored for their varied range of applications such as dye degradation, waste water treatment, anti-microbial, anti-fungal and anti-corrosive activity [8]. Organic inhibitors that contain heteroatoms, such as oxygen, nitrogen, and sulfur are the most efficient chemicals in preventing corrosion. The utilization of organic inhibitors in an acidic solution proves effective in preventing corrosion of carbon steel [9–12]. Mihit et al., conducted research on employing an electrochemical approach and quantum chemical calculations for suppressing the corrosion in copper and zinc in $HNO_3$ solution [13]. Mohamed Kasim Sheit et al. have evaluated the impact of the compound 2-[(*furan-3ylmethylene*)-*amino*]-benzenethiol against the

* Corresponding authors.
*E-mail addresses:* kasimchem1985@gmail.com (H.M.K. Sheit), mohanm.scm.phil@gmail.com (K.S. Mohan).

https://doi.org/10.1016/j.chphi.2024.100521
Received 29 December 2023; Received in revised form 26 January 2024; Accepted 2 February 2024
Available online 3 February 2024

corrosion taking place in carbon steel [14]. Noor et al. have researched the adsorption and consumption restraint influence of N-(l-morphholinobenzyl) on mild steel immersed in an acidic environment [15].

Ade et al. reported the corrosion inhibition efficiency of organic compounds in mild steel exposed to different acidic environments [16]. Ali Ahmed Abdulridha et al. reported the efficiency of the freshly blended Azo Schiff molecule as the erosion inhibitor in carbon steel immersed in a demanding environment of 1 M sulfuric acid. These findings hold practical significance in industries where carbon steel is exposed to acidic solutions, especially in contexts where accurate corrosion prediction is crucial [17]. Sheit et al. have evaluated the anti-corrosive efficacy of 5-Acetyl-3-Phenyl-2,6-Dipyridin-2-Yltetra-Hydropyrimidin-4(1H)−1 inhibitor on mild steel dipped in sodium chloride [18]. Dharmendra Kumar et al. conducted a comprehensive study on imidazole derivatives as inhibitors of corrosion for copper, employing a combined approach involving density functional theory (DFT) and reactive force field methodologies [19]. Bedair et al. have found the potential use of benzidine-based Schiff base compounds as corrosion inhibitors in carbon steel in aqueous HCl of 1.0 M concentration, employing a combination of chemical, electrochemical and computational approaches [20].

Yadav et al. have reported the experimental and theoretical studies on corrosion inhibition effect of synthesized benzothiazole derivatives on mild steel in 15 % HCl solution [21]. Oluwatoba et al. has examined the corrosion inhibition potential of some 2-(4-(substituted) arylidene)−1H-indene-1,3-dione derivatives using density functional theory and molecular dynamics simulation [22]. Khaled et al. investigated the corrosion inhibition in mild steel in acidic media using new oxo-pyrimidine derivatives using experimental and theoretical insights [23]. Ferkous et al. have evaluated the corrosion inhibition in mild steel utilizing 2-(2-methoxybenzylidene) hydrazine-1-carbothioamide in hydrochloric acid solution through experimental measurements and quantum chemical calculations [24]. The present study assesses the effectiveness of the PABN compound as an inhibitor using a diverse set of experimental techniques including weight loss analysis, electrochemical assessments, UV spectroscopy, SEM, EDX, AFM and theoretically using density functional theory (DFT) based quantum calculations.

## 2. Experimental procedure

### 2.1. Preparation of carbon steel specimens

Carbon steel specimens having carbon (0.1 %), sulfur (0.025 %), phosphorus (0.07 %), and the rest containing iron are taken in rectangular form conforming to the standard size of 1.0 cm width, 4.0 cm length, and 0.2 cm thickness. An area of 1 $cm^2$ of the specimen is exposed to electrochemical reactions.

### 2.2. Preparation of stock solution

The process involves the usage of double distilled water and diluted analytical grade $H_2SO_4$ and ethanol for preparing an inhibitor stock solution. The molecular structure of PABN compound is as shown in Fig. 1.

### 2.3. Weight loss analysis

The study quantifies the loss of weight in carbon steel specimens in aqueous solution in the presence and in the absence of PABN inhibitor over a 24-hour period, aiming to determine the compound's inhibition efficiency using the following equation.

$$InhibitionEfficiency\,IE(\%) = \left(\frac{W_o - W_1}{W_o}\right)x100\% \quad (1)$$

$W_0$ represents initial weight of carbon steel without inhibitor; $W_1$ represents weight loss in the presence of inhibitor [25].

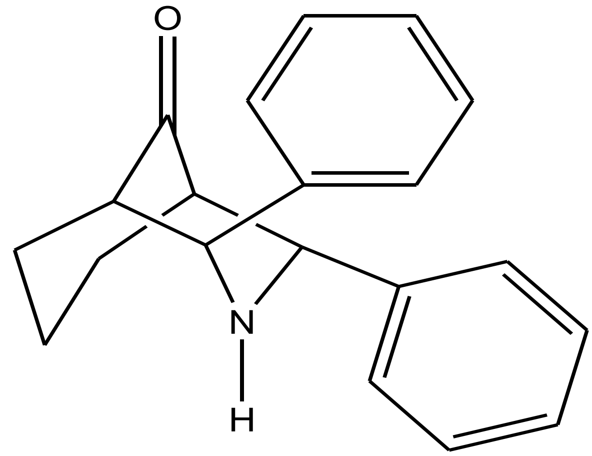

**Fig. 1.** Molecular structure of PABN compound.

### 2.4. Persistence of corrosion rate

Specimens of carbon steel are prepared, weighed up and were suspended in a 100 ml aqueous solution with 0.5 M $H_2SO_4$ and treated with different concentrations of the inhibitor followed by washing, drying and determining the weight again. The corrosion rates are calculated utilizing the following formula.

$$Corrosionrate = \frac{Lossinweight(mg)}{SurfaceareaoftheSpecimen\left(dm^2\right)X\;PeriodofImmersion(days)}mdd \quad (2)$$

### 2.5. Study of potential polarization

Polarization studies were carried out in a three-electrode cell assembly (Fig. 2). The corrosion potential and Tafel slopes are studied by employing CHI660A Electrochemical Workstation Impedance Analyzer. It is a commonly used as a tool for studying corrosion. It uses carbon steel, a saturated calomel electrode and a platinum foil as working electrode, reference standard, and counter electrode respectively as shown in Fig. 2.

### 2.6. Measurement of AC impedance

EIS is a method that uses alternating current potential to measure impedance in an electrochemical system across various frequencies. It provides valuable information about the reaction mechanism, adsorption process, double layer properties and electrode performance aiding in understanding the behavior of the electrochemical system [26]. The $C_{dl}$ value is calculated using the following relation.

$$C_{dl} = \frac{1}{2 \times 3.14 \times R_t \times f_{\max}} \quad (3)$$

### 2.7. Quantum chemical calculations

Density functional theory is utilized for the quantum chemical calculations using B3LYP with electron basis set aug-cc-pvdz for the chosen molecule with Gaussian 16. This investigation resulted in the determination of quantum chemical parameters such as $E_{HOMO}$, $E_{LUMO}$, E(ΔE), dipole moment (μ), chemical hardness (η) and chemical softness (S).

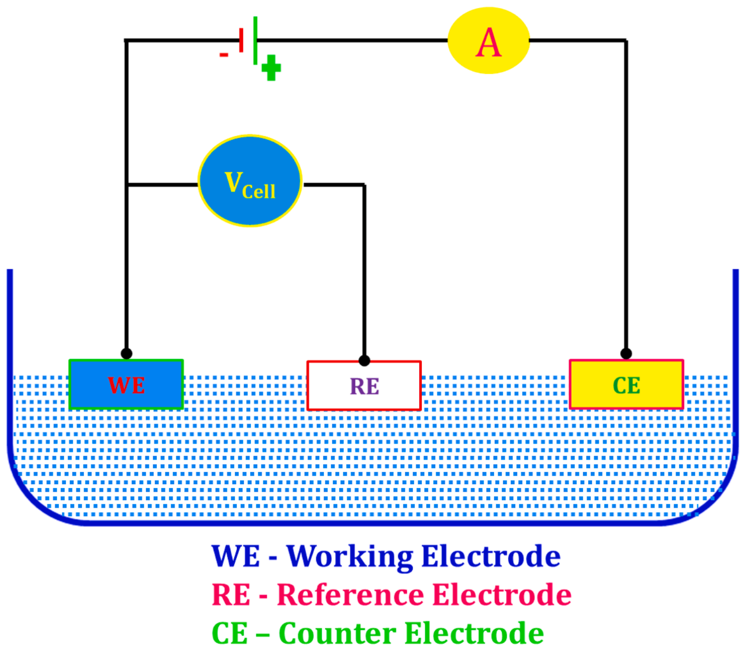


**Fig. 2.** Three-electrode cell assembly.

## 3. Results and discussion

### 3.1. Weight loss method

Table 1 furnishes the values of corrosion rate (CR) and efficiency of inhibition (IE) in carbon steel dipped in 0.5 M $H_2SO_4$ solution derived through weight loss methodology. The compound PABN with a concentration of 0.10 ppm exhibits 97.2 % inhibition efficiency. The IE increases as the concentration of PABN compound increases. The electron-donating feature of oxygen atom and the existence of delocalized π-electrons contribute to the greater inhibition efficiency at higher concentrations of the inhibitor [27]. These characteristics play an important role in enabling the inhibitor to create a protective layer on the surface of carbon steel, thus inhibiting its solubilisation in the acidic solution [28,29].

### 3.2. Potentiodynamic polarization analysis

The polarization investigation confirms the formation of a protective film on the carbon steel surface as a result of corrosion inhibition. This is evident from the decrease in the elevation of linear polarization resistance, reduction in the corrosion current, and a decrease in the corrosion potential. Fig. 3 illustrates the curves of potentiodynamic polarization in carbon steel in 0.5 M $H_2SO_4$ both in the absence and in presence of the inhibitor. Table 2 presents some of the important corrosion factors. In the solution containing 0.5 M $H_2SO_4$, the corrosion potential of carbon steel is -582 mV versus using the Standard Calomel Electrode (SCE). The introduction of PABN compound (0.10 ppm) into the system led to a change in the corrosion potential towards the positive side, measuring -530 mV versus the same SCE. An anodically positioned protective film forms on the surface of carbon steel [30,31]. The film controls the anodic process involved in the dissolution of carbon steel by creating complexes at the anodic locations on the surface of the carbon steel. An increase in the LPR value from 1,569,807.8 ohm cm$^2$ to 2,223,135 ohm cm$^2$ and a reduction in the corrosion current value from 2.970 × $10^{-8}$ A/cm$^2$ to

**Table 1**
Inhibition efficiency at various concentrations of the inhibitor obtained by weight loss method.

| S. No | Concentration of the PABN inhibitor (ppm) | CR (mpy) | Inhibition efficiency (%) |
|---|---|---|---|
| 1 | 0 | 5.478 | 0 |
| 2 | 0.02 | 2.182 | 62.3 |
| 3 | 0.04 | 2.105 | 76.2 |
| 4 | 0.06 | 2.032 | 81.5 |
| 5 | 0.08 | 2.001 | 90.7 |
| 6 | 0.10 | 1.943 | 97.2 |

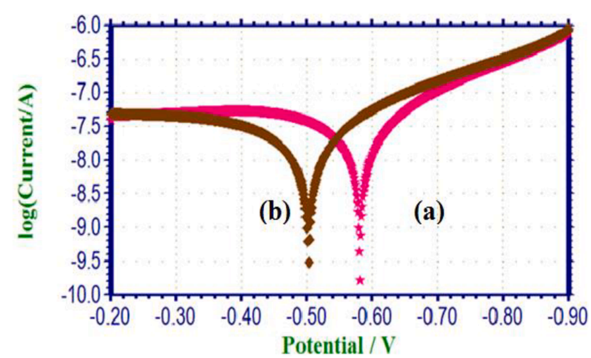


**Fig. 3.** Polarization curves of carbon steel immersed in test solutions (a) Aqueous (0.5 M $H_2SO_4$) + Carbon Steel (b) Aqueous (0.5 M $H_2SO_4$) + Carbon Steel + PABN compound (0.10 ppm).

**Table 2**
Corrosion parameters of carbon steel in an aqueous solution of 0.5 M $H_2SO_4$ in the absence and presence of inhibitor system obtained by potentiodynamic polarization method.

| System | $E_{corr}$(mV vs SCE) | $b_c$(mV/decade) | $b_a$(mV/decade) | LPR (ohm cm$^2$) | $I_{corr}$(A/cm$^2$) |
|---|---|---|---|---|---|
| 0.5 M $H_2SO_4$+ Carbon Steel | −582 | 160 | 326 | 1,569,807.8 | 2.970 × $10^{-8}$ |
| 0.5 M $H_2SO_4$ + Carbon Steel + PABN Inhibitor (0.10 ppm) | −530 | 157 | 309 | 2,223,135 | 2.038 × $10^{-8}$ |

$2.038 \times 10^{-8}$ are witnessed. The polarization analysis validates the establishment of a protective coating on the surface of the carbon steel [32].

### 3.3. AC impedance spectral analysis

The electrochemical impedance spectrum confirms the creation of a protective film on the surface of carbon steel. A protective coating on the carbon steel surface enhances charge transfer resistance, diminishes the double layer capacitance of the specimen and elevates its impedance log. Fig. 4 displays AC impedance spectrum of the specimen made of carbon steel dipped in 0.5 M $H_2SO_4$ in the presence and absence of PABN inhibitor. Table 3 provides the AC impedance parameters obtained from Nyquist plots, encompassing charge transfer resistance ($R_t$) and double layer capacitance ($C_{dl}$) [33]. The addition of PABN compound (0.10 ppm) increases the charge transfer resistance value $R_t$ from 10,309 Ω $cm^{-2}$ to 11,725 Ω $cm^{-2}$, the $C_{dl}$ value decreases from $4.947 \times 10^{10}$ F/$cm^{-2}$ to $4.349 \times 10^{7}$ F/$cm^{-2}$. The impedance value gets incremented from 4.380 to 4.382. The observations suggest the creation of a protective coating on the carbon steel surface [34,35].

### 3.4. UV–Visible spectra analysis

Fig. 5 (a and b) represents the UV–Vis absorption spectra of the sample in a solution containing the molecules of PABN inhibitor. Peaks are observed at 246 nm, 293 nm and 389 nm. Additional peaks at 243 nm and 329 nm appears when PABN solution is added indicating that there is more absorption at these wavelengths. There is an increase in the observed peak intensity also. The alterations that were seen in the spectra, particularly the appearance of new peaks and a rise in intensity, strongly suggest that a complex was formed between the $Fe^{2+}$ ions in the specimen and the 2,4-diphenyl-3-azabicyclo[3.3.1] nonan-9-one molecules that were present in the solution [36]. The creation of a coordination complex is most likely due to the interaction taking place between the $Fe^{2+}$ ions and the organic molecules lying on the surface. It is possible that the development of the complex is because the molecules that were discussed also have the ability to act as ligands and coordinate with the $Fe^{2+}$ ions [37].

### 3.5. SEM and EDX analysis

The details provided in this section outlines the utilization of scanning electron microscopy (SEM) to visually depict the carbon steel specimen's surface in 0.5 M $H_2SO_4$ solution both in the absence and in presence of an inhibitor system. The observations are made from the SEM images presented in Fig. 6 (a–c). In Fig. 6(a), an even and polished surface of carbon steel is evident suggesting that without the exposure to 0.5 M $H_2SO_4$, the carbon steel surface remains corrosion free even after

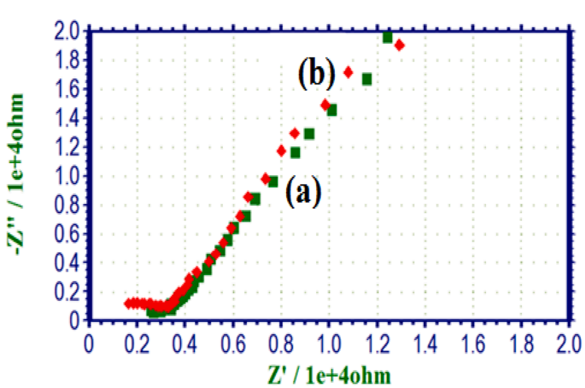


**Fig. 4.** AC impedance spectra (Nyquist plots) of carbon steel immersed in test solutions (a) Aqueous 0.5 M $H_2SO_4$ + Carbon Steel (b) Aqueous 0.5 M $H_2SO_4$ + Carbon Steel + PABN compound (0.10 ppm).

**Table 3**
Corrosion parameters of carbon steel immersed in an aqueous solution containing 0.5 M $H_2SO_4$ in the absence and presence of inhibitor system obtained from AC impedance spectra.

| System | $R_t$(ohm $cm^2$) | $C_{dl}$ (F/ $cm^2$) | Impedance Log (z/ohm) |
|---|---|---|---|
| 0.5 M $H_2SO_4$+ Carbon Steel | 10,309 | $4.947 \times 10^{-10}$ | 4.38 |
| 0.5 M $H_2SO_4$ + Carbon Steel +PABN Inhibitor (0.10 ppm) | 11,725 | $4.349 \times 10^{-10}$ | 4.382 |

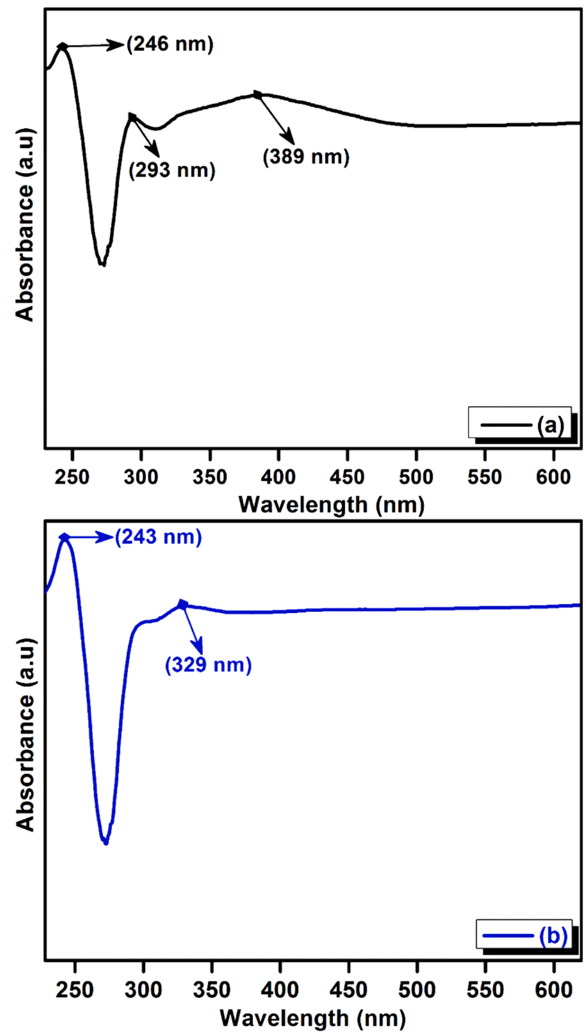


**Fig. 5.** UV-Visible spectrum of solution containing PABN compound (a) without FAS ($Fe^{2+}$) (b) with FAS ($Fe^{2+}$).

one day. Fig. 6(b) shows a rough surface of the carbon steel specimens placed in 0.5 M $H_2SO_4$ solution after a day. The roughness indicates a highly corroded area suggesting that the sulfuric acid solution induces corrosion on the surface of the carbon steel. Fig. 6(c) demonstrates the surface of the specimen in the presence of PABN inhibitor along with the acidic medium, specifically carbon steel + 0.5 M $H_2SO_4$ + 0.10 ppm PABN compound. It is evident that the inhibitor suppresses the rate of corrosion in the specimen. The surface of carbon steel after treating with the inhibitor appears nearly resistant to corrosion [38]. The observed resistance is ascribed to the creation of an intractable complex on its surface serving as a protective film. The SEM images visually support the effectiveness of the PABN inhibitor compound in suppressing the corrosion on the surface of the specimen in the acidic solution [39]. The

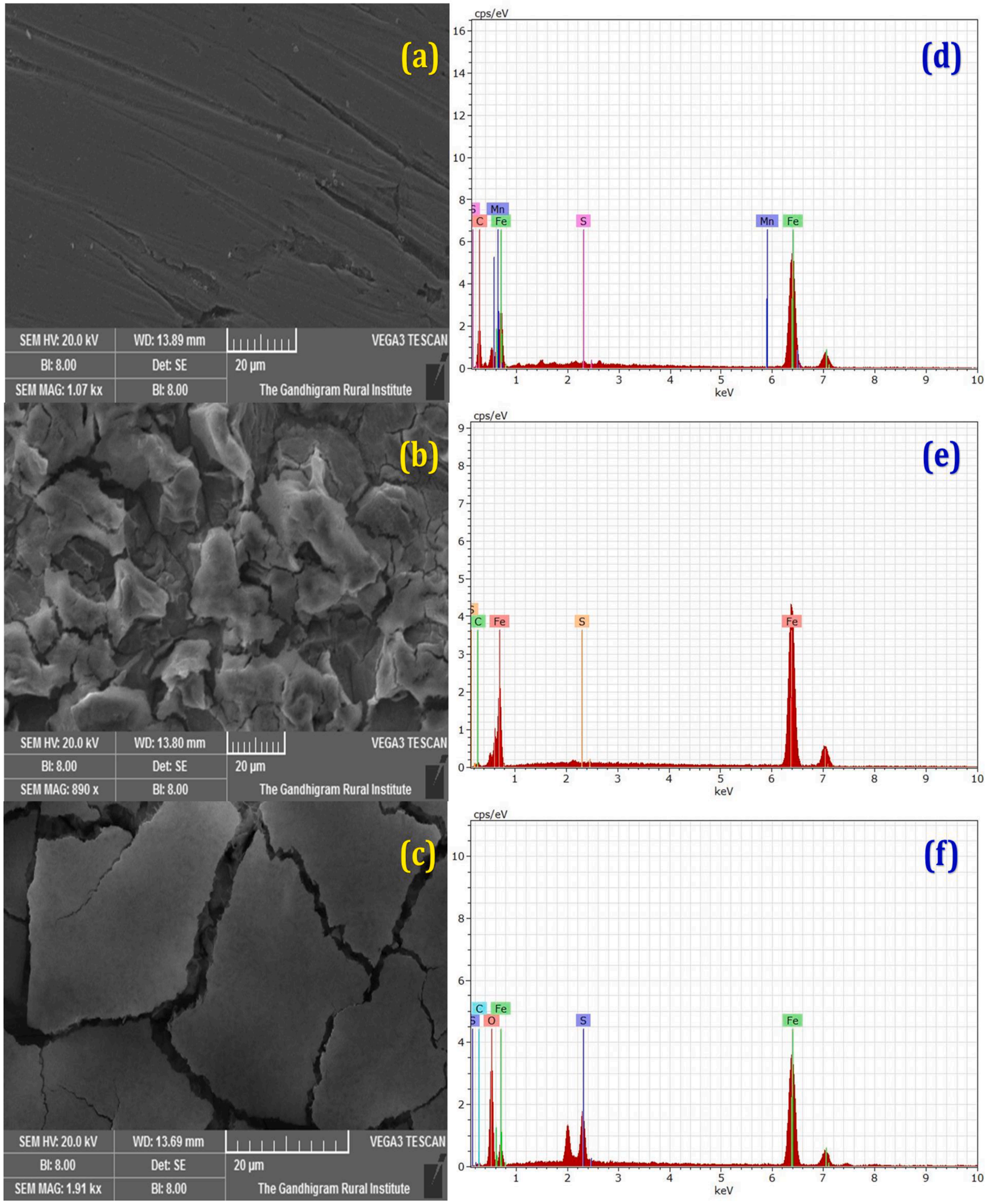


**Fig. 6.** The SEM images and EDX spectrum of (a, d) polished carbon steel surface, (b and e) Aqueous 0.5 M $H_2SO_4$ + Carbon Steel (c and f) Aqueous 0.5 M $H_2SO_4$ + Carbon Steel + PABN compound (0.10 ppm).

inhibitor forms a protective layer, likely an insoluble complex, which inhibits the corrosive effect on the carbon steel [40,41]. Energy dispersive X-ray analyzer was used to analyze the elements on the surface of carbon steel both before and after introducing the PABN inhibitor solution. In Fig. 6 (d, e), the EDX spectrum of the specimen is depicted, illustrating the inherent peaks of the specific elements present in the sample. The EDX spectrum of the sample immersed in 0.5 M $H_2SO_4$ reveals a reduction in carbon related elements suggesting damage caused by the presence of the acid. Fig. 6(f) displays the EDX spectrum of the specimen soaked in $H_2SO_4$ of concentration 0.5 M along with 0.10 ppm of 2, 4- diphenyl-3-azabicyclo[3.3.1] nonan-9-one compound revealing reduced $SO_4$ signal intensity and increased carbon steel peak intensity [42]. An inhibitor causes the appearance of Fe signal and an enhancement of O signal. The data indicates that carbon steel surface is coated with Fe, S, C, and O atoms suggesting an adsorbent inhibitor layer protecting it from corrosion [43]. The research suggests that the adsorption of oxygen (O), nitrogen (N), and carbon (C) atoms from a PABN compound on the surface of carbon steel can result in the formation of a complex resulting in a protective coating.

### 3.6. AFM analysis

Figs. 7 (a-c) presents two-dimensional AFM images depicting the polished metal surface, corroded surface, and film protected metal surface. The corresponding three-dimensional images are also annexed in the same figure. The AFM parameters such as RMS roughness ($R_q$), average roughness ($R_{avg}$), and the value of maximum peak to valley height were calculated and shown in Table 4. The study examined the effect on polished carbon steel specimen and specimen in $H_2SO_4$ of concentration 0.5 M and specimen immersed in PABN inhibitor system along with the acidic medium. In a corrosive environment, carbon steel exhibits an initially elevated average surface roughness [44]. However, the introduction of a 0.10-ppm concentration of the PABN inhibitor compound leads to a subsequent reduction in surface roughness. In the corrosive medium (blank), the average surface roughness of carbon steel is initially high, subsequently decreasing but remaining higher than that of a polished steel surface. The presence of 0.10 ppm of PABN compound results in a smooth defensive layer covering the carbon steel surface affecting all the parameters such as rms value of roughness, peak to valley height, as well as the maximum height of the peak [45,46].

**Table 4**
AFM data for carbon steel immersed in the presence and absence of inhibitor.

| Samples | Value (nm) | | | |
|---|---|---|---|---|
| | $S_p$ | $S_q$ | $S_a$ | $S_y$ |
| Carbon steel surface | 3409.30 | 483.60 | 380.57 | 1753.30 |
| 0.5 M $H_2SO_4$+ Carbon Steel | 2748.30 | 380.13 | 294.72 | 2687.70 |
| 0.5 M $H_2SO_4$ + Carbon Steel + PABN Inhibitor (0.10 ppm) | 2272.30 | 310.42 | 245.73 | 1218.50 |

### 3.7. The density functional theory approach

Surface adsorption causes corrosion inhibition but correlation between the corrosion inhibition and PABN molecular properties are not explored. DFT studies are employed to analyze the inhibitor's electronic and geometrical structure. It reveals increased binding efficiency with higher HOMO and lower LUMO energy values [47]. The molecule's high chemical activity and low kinetic stability are attributed to its increased polarizing power due to its minimized energy gap [48]. Fig. 8 illustrates the orbital density distribution of frontier molecules with oxygen atoms having a high electron density potentially forming adsorption active

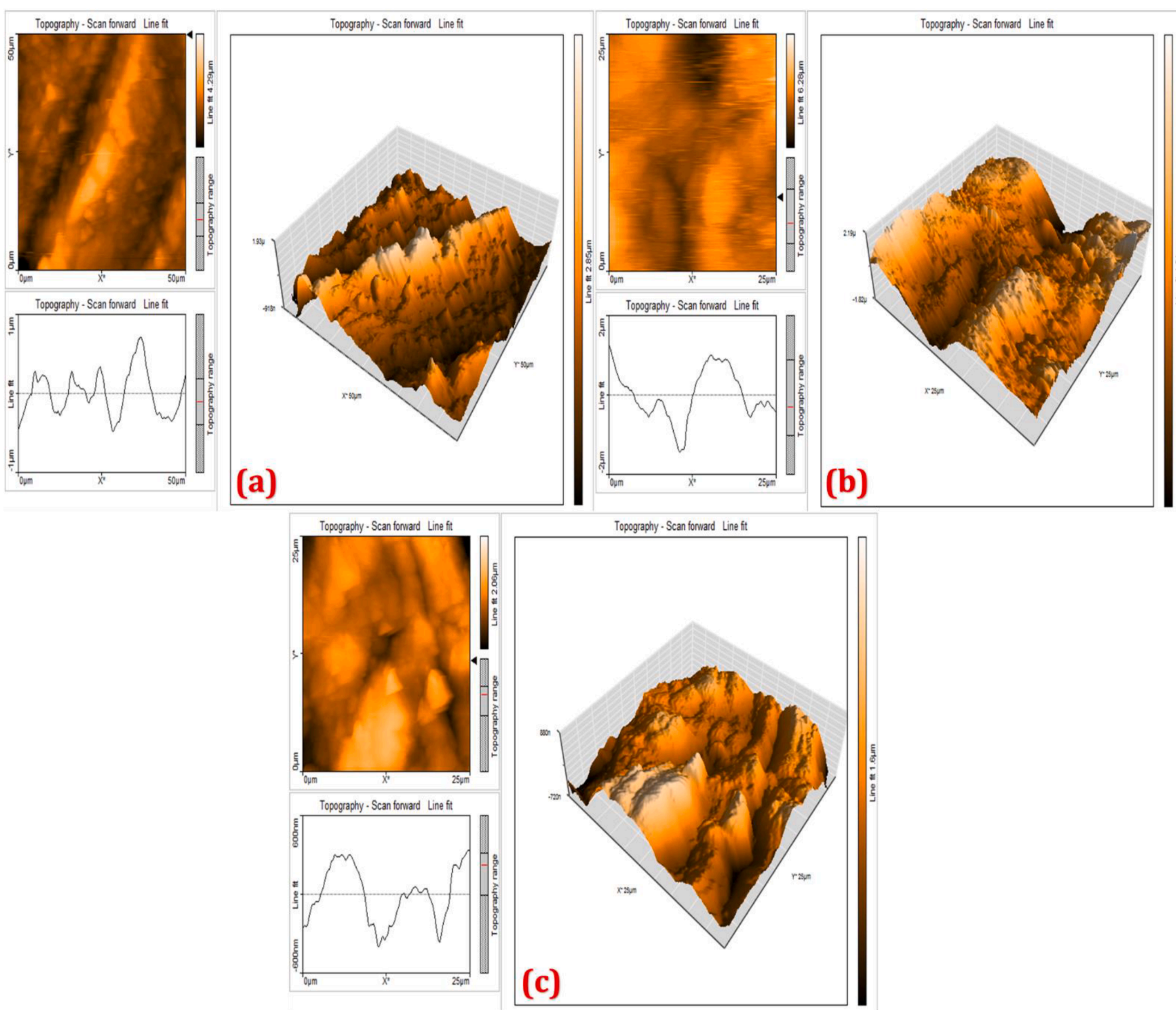


**Fig. 7.** AFM cross sectional image of (a) polished carbon steel surface (control), (b) Carbon steel surface after immersion in 0.5 M $H_2SO_4$ (blank), (c) Carbon steel surface after immersion 0.5 M $H_2SO_4$+ 0.10 ppm of PABN compound.

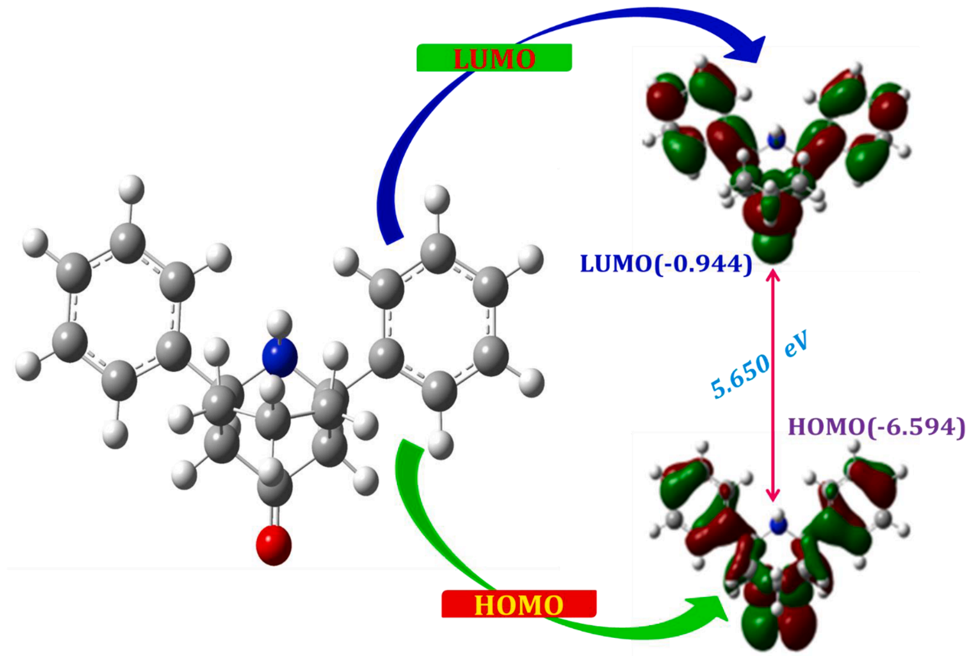


**Fig. 8.** HOMO and LUMO electron density of PABN compound.

centres. The analysis indicates that a higher occupied molecular orbital (HOMO) inhibitor (−6.594 eV) enhances the metal's ability to provide electrons to its unoccupied orbital, thereby improving its corrosion inhibition efficiency [49]. Lower unoccupied molecular orbital LUMO (−0.944 eV) accepts electrons from metal surfaces, improving inhibitor efficiency as the energy gap between HOMO and LUMO decreases (5.650 eV). The lower dipole moment value of PABN compound indicates a less polar favourable interaction with metal surfaces potentially acting as a corrosion inhibitor [50].

## 4. Conclusion

The current research indicates that 2, 4-diphenyl-3-azabicyclononan-9-one shows promise as an effective corrosion inhibitor in carbon steel in a 0.5 M $H_2SO_4$ environment. The protective film of the inhibitor compound shows a 97.2 % efficiency in controlling carbon steel corrosion in the afore mentioned acidic environment. The compound effectively prevents corrosion by acting as an anodic inhibitor affecting the anodic reactions that lead to corrosion. The polarization study reveals an augmented charge transfer resistance along with a reduction in double layer capacitance and corrosion current. These observations imply that the presence of an adsorbed layer contributes to the creation of a protective coating. UV–visible spectra confirm the protective film's presence with $Fe^{2+}$ ions an inhibiting material while microscopic analysis reveals a smoother surface. Density functional theory approach is highly accurate in predicting inhibitor efficiency due to its consistent match with the experimental results.

## Competing interest

On behalf of all authors the corresponding author states that there is no conflict of interest.

## Funding acknowledgement

The authors declare that no funds, grants, or any other support was received during the work and preparation of this manuscript.

## CRediT authorship contribution statement

**H. Mohamed Kasim Sheit:** Writing – review & editing, Writing – original draft, Validation, Supervision, Methodology, Investigation, Formal analysis. **K.S. Mohan:** Writing – review & editing, Writing – original draft, Validation, Software, Investigation, Formal analysis. **K.V. Gunavathy:** Writing – review & editing, Writing – original draft, Validation, Software, Formal analysis. **S.S. Syed abuthahir:** Writing – review & editing, Validation. **M. Varusai Mohamed:** Writing – review & editing. **P. Subhapriya:** Writing – review & editing, Writing – original draft, Validation. **A. Samsathbegum:** Writing – review & editing. **G . Hema Sindhuja:** Writing – review & editing.

## Declaration of competing interest

The authors declare that they have no known competing financial interests or personal relationships that could have appeared to influence the work reported in this paper.

The authors declare that no competing financial interests.

## Data availability

No data was used for the research described in the article.

## Acknowledgment

The authors are thankful to the Principal and the college management committee members of Jamal Mohamed College (Autonomous) for providing necessary facilities.

## References

[1] A. Kistan, S. Mohan, S. Mahalakshmi, A. Jayanthi, A. Ramya, Janaki, P.S. Karthik, Sol-Gel technique, characterization and photocatalytic degradation activity of Manganese doped ZnO nanoparticles, Main Group Chem. 24 (4) (2023) 1–14, https://doi.org/10.3233/MGC-230067.

[2] K. Andiyappan, R. Sathiyamoorthi, Intensification of Bio-synthesis of Zirconium Oxide ($ZrO_2$) nanoparticles derived from novel CrescentiaCujete fruits: effects on diesel engine characteristics powered by Waste Engine oil methyl ester-Diesel

blend, Chem. Eng. Process. Process Intensif. (2023) 109642, https://doi.org/10.1016/j.inoche.2023.111942.

[3] U.M. Nisha, D. Venkatesh, S. Arulmurugan, A. Kistan, P. Rajeshwaran, P. Siva Karthik, Assessment of solar light sensitive Chitosan integrated CeO2-CuO ternary composites for the efficient degradation of malachite green, acid blue 113 dyes and microbial studies, Inorg. Chem. Commun. (2023) 111942, https://doi.org/10.1016/j.inoche.2023.111942.

[4] A. Kistan, V. Kanchana, Silver-alumina impregnated maghemite/magnetite nanocomposites for effective removal of chromium(VI) from the tannery discharge, Asian J. Chem. 35 (8) (2023) 1899–1906, https://doi.org/10.14233/ajchem.2023.27792.

[5] A. A. Kistan, A. Premkumar, V. Kanchana, A Simple treatment of tannery wastewater using modified activated carbon by metal chloride Asian J. Chem 34 (7) (2022) 1698–1702, https://doi.org/10.14233/ajchem.2022.23699.

[6] A. Kistan, V. Kanchana, L. Sakayasheela, J. Sumathi, A. Premkumar, A. Selvam, Titanium dioxide as a catalyst for photodegradation of various concentrations of methyl orange and methyl red dyes using Hg vapour lamp with constant pH, Orient. J. Chem. 34 (2) (2018), https://doi.org/10.13005/ojc/340250.

[7] V.A.V. Alagarsamy, K. Andiyappan, S. Abdul Kadar Avuliya, T.A. Abubacker, Retarding of preliminary chemical pollutants from dye effluent by metal nano particles synthesized using flower extract of catharanthusroseus, Orient. J. Chem. 34 (1) (2018) 381, https://doi.org/10.13005/ojc/340141.

[8] S.N. Costa, F.W.Q. Almeida-Neto, O.S. Campos, T.S. Fonseca, M.C. Mattos, V. N. Freire, P. Homem-de-Mello, E.S. Marinho, N.K.V. Monteiro, A.N. Correia, P. Lima-Neto, Carbon steel corrosion inhibition in acid medium by imidazole-based molecules: experimental and molecular modelling approaches, J. Mol. Liq. 326 (2021) 115330, https://doi.org/10.1016/j.molliq.2021.115330.

[9] K.S.M. V.Rathi, A.S. R.Sathiyapriya, Improved visible light response photocatalytic activity of $CuWO_4$/g-$C_3N_4$ nanocomposites for degradation of organic dyes, J. Mater. Sci.: Mater. Electron. 34 (22) (2023) 1629, https://doi.org/10.1007/s10854-023-10996-5.

[10] K.K. Anupama, K. Ramya, A. Joseph, Electrochemical measurements and theoretical calculations on the inhibitive interaction of plectranthusamboinicus leaf extract with carbon steel in hydrochloric acid, Measurement 95 (2017) 297–305, https://doi.org/10.1016/j.measurement.2016.10.030.

[11] T.A. Onat, D. Yiğit, H. Nazır, M. Güllü, G. Dönmez, Bio corrosion inhibition effect of 2-amino pyrimidine derivatives on SRB, Int. J. Corros. Scale Inhib 5 (3) (2016) 273–281, https://doi.org/10.17675/2305-6894-2016-5-3-1.

[12] A. Dehghani, G. Bahlakeh, B. Ramezanzadeh, M. Ramezanzadeh, Potential role of a novel green eco-friendly inhibitor in corrosion inhibition of carbon steel in HClsolution:detailed macro/micro-scale experimental and computational explorations, Constr. Build. Mater. 245 (2020) 118464, https://doi.org/10.1016/j.conbuildmat.2020.118464.

[13] M. Mihit, K. Laarej, H. Abou El Makarim, L. Bazzi, R. Salghi, B. Hammouti, Study of the inhibition of the corrosion of copper and zinc in $HNO_3$ solution by electrochemical technique and quantum chemical calculations, Arab. J. Chem. 3 (1) (2010) 55–60.

[14] H. Mohamed KasimSheit, S. MusthafaKani, M. Anwar Sathiq, S.S. Syed Abuthahir, K.S. Mohan, S. Berbeth Mary, K.V. Gunavathy, Investigations on the effect of 2-[(*furan-3ylmethylene*)-*amino*]-benzenethiol on corrosion in carbon steel, Results Surf. Interfaces 12 (2023) 100143, https://doi.org/10.1016/j.rsurfi.2023.100143.

[15] E.A. Noor, Adsorption and corrosion inhibition effect of N – (l Morpholinobenzyl) urea on mild steel in acidic medium, Corros. Sci. 47 (2005) 33–35, https://doi.org/10.1155/2011/892548.

[16] S.B. Ade, Corrosion inhibition of mild steel in different acid medium by using various acidic groups of organic compounds, Int. J. Res. Appl. Sci. Eng. Technol. 10 (2) (2022) 367–373, https://doi.org/10.22214/ijraset.2022.40288.

[17] A.A. Abdulridha, M.A.A.H. Allah, S.Q. Makki, Y. Sert, H.E. Salman, A.A. Balakit, Corrosion inhibition of carbon steel in 1M $H_2SO_4$ using new Azo Schiff compound: electrochemical, gravimetric, adsorption, surface and DFT studies, J. Mol. Liq. 315 (2020) 113690, https://doi.org/10.1016/j.molliq.2020.113690.

[18] H.M.K. Sheit, M.S. Mubarak, G. Benitta, Anti-corrosive efficiency of mild steel in sodium chloride solution using 5-acetyl-3-phenyl-2, 6-dipyridin-2-yltetra-hydropyrimidin-4(1H)-1 compound as an inhibitor, J. Bio Tribocorros. 8 (2022) 103, https://doi.org/10.1007/s40735-022-00703-y.

[19] D. Kumar, V. Jain, B. Rai, Imidazole derivatives as corrosion inhibitors for copper: a DFT and reactive force field study, Corros. Sci. 171 (2020) 108724, https://doi.org/10.1016/j.corsci.2020.108724.

[20] M.A. Bedair, S.A. Soliman, MF. Bakr, E.S. Gad, I-M.C Hassanelgaz, M. Salama, FZ. Alqahtany, Benzidine-based Schiff base compounds for employing as corrosion inhibitors for carbon steel in 1.0M HCl aqueous media by chemical, electrochemical and computational methods, J. Mol. Liq. 317 (2020) 114015, https://doi.org/10.1016/j.molliq.2020.114015.

[21] M. Yadav, S. Kumar, N. Kumari, I. Bahadur, E. Ebenso, Experimental and theoretical studies on corrosion inhibition effect of synthesized benzothiazole derivatives on mild steel in 15% HCl solution, Int. J. Electrochem. Sci. 10 (2015) 602–624, https://doi.org/10.1016/S1452-3981(23)05017-4.

[22] O.E. Oyeneyin, N.D. Ojo, N. Ipinloju, et al., Investigation of the corrosion inhibition potentials of some 2-(4-(substituted) arylidene)-1H-indene-1,3-dione derivatives: density functional theory and molecular dynamics simulation, Beni Suef Univ. J. Basic Appl. Sci. 11 (2022) 132, https://doi.org/10.1186/s43088-022-00313-0.

[23] K.S.M. Ferigita, M. Saracoglu, M.G.K. AlFalah, M.I. Yilmazer, Z. Kokbudak, S. Kaya, F. Kandemirli, Corrosion inhibition of mild steel in acidic media using new oxo-pyrimidine derivatives: experimental and theoretical insights, J. Mol. Struct. 1284 (2023) 135361, https://doi.org/10.1016/j.molstruc.2023.135361.

[24] H. Ferkous, S. Djellali, R. Sahraoui, Y. Benguerba, H. Behloul, A. Çukurovali, Corrosion inhibition of mild steel by 2-(2-methoxybenzylidene) hydrazine-1-carbothioamide in hydrochloric acid solution: experimental measurements and quantum chemical calculations, J. Mol. Liq. 307 (2020) 112957, https://doi.org/10.1016/j.molliq.2020.112957.

[25] S. Rajendran, R. Srinivasan, R. Dorothy, T. Umasankareswari, A. Al-Hashem, Green solution to corrosion problems-at a glance, Int. J. Corros. Scale Inhib. 8 (3) (2019) 437–479, https://doi.org/10.17675/2305-6894-2019-8-3-1.

[26] A. Saxena, D. Prasad, R. Haldhar, G. Singh, A. Kumar, Use of Saracaashoka extract as green corrosion inhibitor for carbon steel in 0.5M $H_2SO_4$, J. Mol. Liq. 258 (2018) 89–97, https://doi.org/10.1016/j.molliq.2018.02.104.

[27] M.E.A.L.D. R.J.Tuama, M.N. Khalaf, Recycling and evaluation of poly (ethylene terephthalate) waste as effective corrosion inhibitors for C-steel material in acidic media, Int. J. Corros. Scale Inhib. 9 (2) (2020) 427–445, https://doi.org/10.17675/2305-6894-2020-9-2-3.

[28] P.A. Jeeva, G.S. Mali, R. Dinakaran, K. Mohanam, S. Karthikeyan, The influence of Co-Amoxiclav on the corrosion inhibition of carbon steel in 1N hydrochloric acid solution, Int. J. Corros. Scale Inhib. 8 (1) (2019) 1–12, https://doi.org/10.17675/2305-6894-2019-8-1-1.

[29] S. Shahabi, S. Hamidi, J.B. Ghasemi, P. Norouzi, A. Shakeri, Synthesis, experimental, quantum chemical and molecular dynamics study of carbon steel corrosion inhibition effect of two Schiff bases in HCl solution, J. Mol. Liq. 285 (2019) 626–639, https://doi.org/10.1016/j.molliq.2019.04.137.

[30] C.M. Fernandes, V.G. Pina, L.X. Alvarez, A.C.F. de Albuquerque, F.M. dos Santos Júnior, A.M. Barrios, J.A. Velasco, E.A. Ponzio, Use of a theoretical Prediction method and quantum chemical calculations for the design, synthesis and experimental evaluation of three green corrosion inhibitors for carbon steel, Colloids Surf. A 599 (2020) 124857, https://doi.org/10.1016/j.colsurfa.2020.124857. Physicochemical and Engineering Aspects.

[31] M. Anwar Sathiq, A. Jamal Abdul Nasser, P. Mohamed Sirajudeen, Adsorption and corrosion inhibition effect of N-(l-Morpholinobenzyl) urea on mild steel in acidic medium, E J. Chem. 8 (2) (2011) 621–628, https://doi.org/10.1155/2011/892548.

[32] A.G. Baby, S. Rajendran, V. Johnsirani, A. Al-Hashem, N. Karthiga, P. Nivetha, Influence of zinc sulphate on the corrosion resistance of L80 alloy immersed in seawater in the absence and presence of sodium potassium tartrate and trisodium citrate, Int. J. Corros. Scale Inhib 9 (3) (2020) 979–999, https://doi.org/10.17675/2305-6894-2020-9-3-12.

[33] N.Z.N. Hashim, K. Kassim, H.M. Zaki, A.I. Alharthi, Z. Embong, X.P.S. and, DFT investigations of corrosion inhibition of substituted benzylidene Schiff bases on carbon steel in hydrochloric acid, Appl. Surf. Sci. 476 (2019) 861–877, https://doi.org/10.1016/j.apsusc.2019.01.149.

[34] H. Ferkous, S. Djellali, R. Sahraoui, Y. Benguerba, H. Behloul, A. Çukurovali, Corrosion inhibition of mild steel by 2-(2-methoxybenzylidene) hydrazine-1-carbothioamide in hydrochloric acid solution: experimental measurements and quantum chemical calculations, J. Mol. Liq. 307 (2020) 112957, https://doi.org/10.1016/j.molliq.2020.112957.

[35] A. Acidi, A. Sedik, A. Rizi, R. Bouasla, K.O. Rachedi, M. Berredjem, Y. Bengureba, Examination of the main chemical components of essential oil of Syzygiumaromaticum as a corrosion inhibitor on the mild steel in 0.5M HCl medium, J. Mol. Liq. 391 (2023) 123423, https://doi.org/10.1016/j.molliq.2023.123423.

[36] M. Alahiane, R. Oukhrib, Y.A. Albrimi, H. AbouOualid, R. Idouhli, A. Nahlé, M. &Hamdani, Corrosion inhibition of SS 316L by organic compounds: experimental, molecular dynamics, and conceptualization of molecules–surface bonding in $H_2SO_4$ solution, Appl. Surf. Sci. 612 (2023) 155755, https://doi.org/10.1016/j.apsusc.2022.155755.

[37] N.A. Wazzan, I.B. Obot, S. Kaya, Theoretical modelling and molecular level insights into the corrosion inhibition activity of 2-amino-1, 3, 4-thiadiazole and its 5-alkyl derivatives, J. Mol. Liq. 221 (2016) 579–602, https://doi.org/10.1016/j.molliq.2016.06.011.

[38] F. Liu, L. Chen, Thiadiazoles as potent inhibitors against corrosion of metals and alloys: challenges and future prospects, J. Mol. Liq. (2023) 122904, https://doi.org/10.1016/j.molliq.2023.122904.

[39] R.M K.S.Mohan, Y. Shin, V.B K.V.Gunavathy, M. Ubaidullah, M. Shkir, V.R. M. Reddy, W.K. Kim, Substrate heat-assisted spray pyrolysis of crack-free ytterbium sesquioxide-Si heterojunction diodes for photo-sensing applications, Surf. Interfaces 39 (2023) 102887, https://doi.org/10.1016/j.surfin.2023.102887.

[40] A.A. Alamiery, Anticorrosion effect of thiosemicarbazide derivative on mild steel in 1M hydrochloric acid and 0.5M sulfuric acid: gravimetrical and theoretical studies, Mater. Sci. Energy Technol. 4 (2021) 263–273, https://doi.org/10.1016/j.mset.2021.07.004.

[41] K.S. Mohan, A. Panneerselvam, R. Marnadu, J. Chandrasekaran, M. Shkir, A. Tataroglu, A systematic influence of Cu doping on structural and opto-electrical properties of fabricated $Yb_2O_3$ thin films for Al/Cu-$Yb_2O_3$/p-Si Schottky diode applications, Inorg. Chem. Commun. 129 (2021) 108646, https://doi.org/10.1016/j.inoche.2021.108646.

[42] N.O. Obi-Egbedi, K.E. Essien, I.B. Obot, E. Ebenso, E, 1, 2-Diaminoanthraquinone as corrosion inhibitor for mild steel in hydrochloric acid: weight loss and quantum chemical study, Int. J. Electrochem. Sci. 6 (4) (2011) 913–930, https://doi.org/10.1016/S1452-3981(23)15045-0.

[43] C. Zhang, H. Duan, J. Zhao, Synergistic inhibition effect of imidazoline derivative and L-cysteine on carbon steel corrosion in a $CO_2$-saturated brine solution, Corros. Sci. 112 (2016) 160–169, https://doi.org/10.1016/j.corsci.2016.07.018.

[44] K.S. Mohan, A. Panneerselvam, J. Chandrasekaran, et al., An in-depth examination of opto-electrical properties of In-$Yb_2O_3$ thin films and fabricated Al/In-$Yb_2O_3$/p-Si

(MIS) hetero junction diodes, Appl. Nanosci. 11 (2021) 1617–1635, https://doi.org/10.1007/s13204-021-01817-4.

[45] H.H. Zhang, X. Pang, M. Zhou, C. Liu, L. Wei, K. &Gao, The behavior of pre-corrosion effect on the performance of imidazoline-based inhibitor in 3wt.%NaCl solution saturated with $CO_2$, Appl. Surf. Sci. 356 (2015) 63–72, https://doi.org/10.1016/j.apsusc.2015.08.003.

[46] A. Panneerselvam, K.S. Mohan, R. Marnadu, et al., The deep investigation of structural and opto-electrical properties of $Yb_2O_3$ thin films and fabrication of Al/$Yb_2O_3$/p-Si (MIS) Schottky barrier diode, J. Sol Gel Sci Technol 102 (2022) 597–613, https://doi.org/10.1007/s10971-021-05683-y.

[47] A. Aouniti, M. El Azzouzi, I. Belfilali, I.K. Warad, H. Elmsellem, B. Hammouti, A. Zarrouk, Anticorrosion potential of new synthesized naphtamide on mild steel in hydrochloric acid solution: gravimetric, electrochemical, surface morphological, UV–visible and theoretical investigations, Anal. Bioanal. Electrochem. 10 (9) (2018) 1193–1210.

[48] S.M. Shaban, N-(3-(Dimethyl benzyl ammonio) propyl) alkanamide chloride derivatives as corrosion inhibitors for mild steel in 1M HCl solution: experimental and theoretical investigation, RSC. Adv. 6 (46) (2016) 39784–39800, https://doi.org/10.1039/C6RA00252H.

[49] A. Berrissoul, A. Ouarhach, F. Benhiba, A. Romane, A. Zarrouk, A. Guenbour, A. Dafali, Evaluation of Lavandulamairei extract as green inhibitor for mild steel corrosion in 1M HCl solution. Experimental and theoretical approach, J. Mol. Liq. 313 (2020) 113493, https://doi.org/10.1016/j.molliq.2020.113493.

[50] S. Nikpour, M. Ramezanzadeh, G. Bahlakeh, B. Ramezanzadeh, M. Mahdavian, Eriobotrya japonica Lindl leaves extract application for effective corrosion mitigation of mild steel in HCl solution: experimental and computational studies, Constr. Build. Mater. 220 (2019) 161–176, https://doi.org/10.1016/j.conbuildmat.2019.06.005.